MODELING THE EARTH'S IONOSPHERE: SAMI2 AND RF HEATING

J.D. Huba
Plasma Physics Division
Naval Research Laboratory
Washington, DC

RF Ionospheric Interactions Workshop
Santa Fe, NM

18 April 2010

Acknowledge: G. Joyce, M. Swisdak and P. Bernhardt

SAMI2 OPEN SOURCE PROJECT

http://wwwppd.nrl.navy.mil/sami2-OSP/index.html

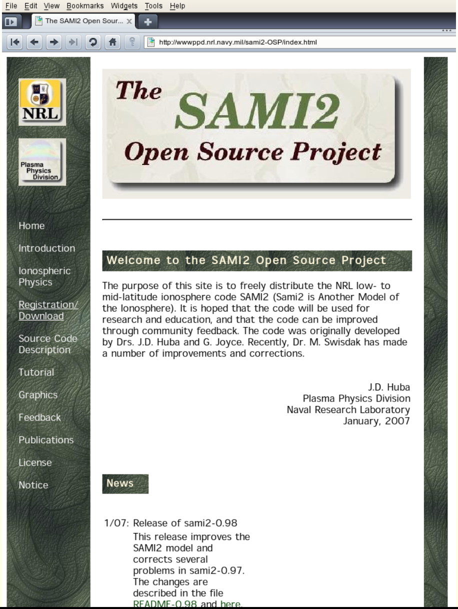

- overview of SAMI2 model
  - basic equations
  - physical inputs
  - numerical methods
- application to RF heating
  - code modification
  - examples: sura/arecibo

WHAT ARE THE INGREDIENTS?

- plasma dynamics
- neutral atmosphere
- photoionization
- chemistry
- magnetic field
- electric field

PLASMA DYNAMICS

- ion continuity

$$\frac{\partial n_i}{\partial t} + \nabla \cdot (n_i \mathbf{V}_i) = P_i - L_i n_i$$

- ion velocity

$$\frac{\partial \mathbf{V}_i}{\partial t} + \mathbf{V}_i \cdot \nabla \mathbf{V}_i = -\frac{1}{\rho_i} \nabla \mathbf{P}_i + \frac{e}{m_i} \mathbf{E} + \frac{e}{m_i c} \mathbf{V}_i \times \mathbf{B} + \mathbf{g}$$

$$-\nu_{in} (\mathbf{V}_i - \mathbf{V_n}) - \sum_j \nu_{ij} \left(\mathbf{V}_i - \mathbf{V}_j \right)$$

- ion temperature

$$\frac{\partial T_i}{\partial t} + \mathbf{V}_i \cdot \nabla T_i + \frac{2}{3} T_i \nabla \cdot \mathbf{V}_i + \frac{2}{3} \frac{1}{n_i k} \nabla \cdot \mathbf{Q}_i = Q_{in} + Q_{ij} + Q_{ie}$$

PLASMA DYNAMICS

- electron momentum

$$0 = -\frac{1}{n_e m_e} b_s \frac{\partial P_e}{\partial s} - \frac{e}{m_e} E_s$$

- electron temperature

$$\frac{\partial T_e}{\partial t} - \frac{2}{3}\frac{1}{n_e k} b_s^2 \frac{\partial}{\partial s}\kappa_e \frac{\partial T_e}{\partial s} = Q_{en} + Q_{ei} + Q_{phe} + Q_{RF}$$

NEUTRAL ATMOSPHERE

- dominant species:
  - atomic: H, He, N, O
  - molecular: N_2, NO, O_2
- neutral density scale height:

$$H = kT/mg$$

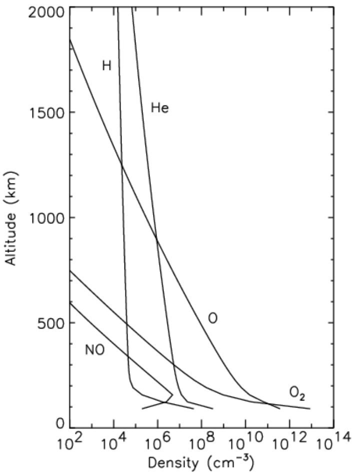

NEUTRAL ATMOSPHERE MODELS

- empirical models
  - NLRMSISE-00 (*Picone et al.*)
    provides neutral densities and temperature
  - HWM93/HWM07 (*Hedin/Drob*)
    provides neutral wind
- first principle models
  - NCAR TIME-GCM (*Roble/Crowley*)
  - CTIP (*Fuller-Rowell*)

PHOTOIONIZATION

- dominant production mechanism for ionospheric plasma
- solar X-ray (1 – 170 Å) and EUV (170 – 1750 Å) radiation can ionize the ionosphere neutral gas

Species	IP (ev)	λ (Å)
H	13.6	912
He	24.6	504
N	14.5	853
O	13.6	911
N_2	15.6	796
NO	9.3	1340
O_2	10.1	1027

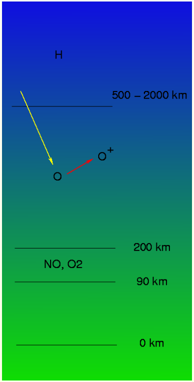

PHOTOIONIZATION: CALCULATION

- production (P) needs to be calculated
- continuity equation for ion species X^+

$$dX^+/dt = P_{X^+} = n_n(X) I_R \quad \text{where}$$

$$P_X = n_n(X) \sum_\lambda \underbrace{\sigma_X^{(i)}(\lambda)}_{\text{photoionization}} \underbrace{\exp\left[- \sum_m \sigma_m^{(a)}(\lambda) \int_z^\infty n_m(s)\, ds \right]}_{\text{photoabsorption}} \underbrace{\phi_\infty(\lambda)}_{\text{solar flux}}$$

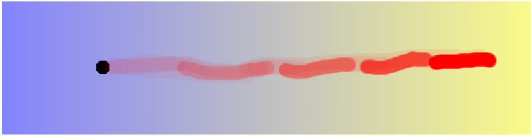

PHOTOIONIZATION: SOLAR FLUX MODELS

- empirical models: flux $\phi_\infty(\lambda)$ is in 37 wavelength bins
  - Hinteregger
  - Torr and Torr
  - EUVAC (*Richards et al.*, 1994)
    function of geophysical conditions
    $\phi_i = F74113_i[1 + A_i(P - 80)]$ where
    $P = (F10.7A + F10.7)/2$
- data/model driven
  - NRLEUV (*Lean, Warren, and Mariska*)
  - SOLAR2000 (*Tobiska*)
  - FISM (*Chamberlin*)
- photoionization/photoabsorption cross-sections tabulated

CHEMISTRY

- production (P) and loss (L) mechanism
- continuity equations for ion species X^+ and Y^+

$$dX^+/dt = P_{X^+} - L_{X^+} \quad \text{(e.g., } dH^+/dt = P_{H^+} - L_{H^+}\text{)}$$
$$dY^+/dt = P_{Y^+} - L_{Y^+} \quad \text{(e.g., } dO^+/dt = P_{O^+} - L_{O^+}\text{)}$$

- general chemical reaction (e.g., charge exchange)

$$X^+ + Y \rightarrow X + Y^+ \quad \mathrm{Rate}: k_{X+Y}$$
$$\text{(e.g., } H^+ + O \rightarrow H + O^+ \quad \mathrm{Rate}: k_{H+O}\text{)}$$

- thus, in continuity use

$$L_{X^+} = P_{Y^+} = k_{X+Y} n(X^+) n(Y)$$
$$\text{(e.g., } L_{H^+} = P_{O^+} = k_{H+O} n(H^+) n(O)\text{)}$$

CHEMICAL REACTION RATES

Chemical Reaction Rates:

Reaction	Rate, $cm^3 s^{-1}$
$H^+ + O \rightarrow O^+ + H$	$2.2 \times 10^{-11} T^{0.5}(H^+)$
$He^+ + N_2 \rightarrow N_2{}^+ + He$	3.5×10^{-10}
$He^+ + N_2 \rightarrow N^+ + N + He$	8.5×10^{-10}
$He^+ + O_2 \rightarrow O^+ + O + He$	8.0×10^{-10}
$He^+ + O_2 \rightarrow O_2{}^+ + He$	2.0×10^{-10}
$N^+ + O_2 \rightarrow NO^+ + O$	2.0×10^{-10}
$N^+ + O_2 \rightarrow O_2{}^+ + N(2D)$	4.0×10^{-10}
$N^+ + O \rightarrow O^+ + N$	1.0×10^{-12}
$N^+ + NO \rightarrow NO^+ + O$	2.0×10^{-11}
$O^+ + H \rightarrow H^+ + O$	$2.5 \times 10^{-11} T_n^{0.5}$
$O^+ + N_2 \rightarrow NO^+ + N$	k_1
$O^+ + O_2 \rightarrow O_2{}^+ + O$	k_2
$O^+ + NO \rightarrow NO^+ + O$	1.0×10^{-12}
$N_2{}^+ + O \rightarrow NO^+ + N(2D)$	$1.4 \times 10^{-10} T_{300}^{-0.44}(O+)$
$N_2{}^+ + O_2 \rightarrow O_2{}^+ + N_2$	$5.0 \times 10^{-11} T_{300}^{-0.5}(O+)$
$N_2{}^+ + O_2 \rightarrow NO^+ + NO$	1.0×10^{-14}
$N_2{}^+ + NO \rightarrow NO^+ + N_2$	3.3×10^{-10}
$O_2{}^+ + N \rightarrow NO^+ + O$	1.2×10^{-10}
$O_2{}^+ + N(2D) \rightarrow N^+ + O_2$	2.5×10^{-10}
$O_2{}^+ + NO \rightarrow NO^+ + O_2$	4.4×10^{-10}
$O_2{}^+ + N_2 \rightarrow NO^+ + NO$	5.0×10^{-16}

Recombination Rates:

Reaction	Rate, $cm^3\ s^{-1}$
$H^+ + e \rightarrow H$	$4.43 \times 10^{-12}/T_e^{0.7}$
$He^+ + e \rightarrow He$	$4.43 \times 10^{-12}/T_e^{0.7}$
$N^+ + e \rightarrow N$	$4.43 \times 10^{-12}/T_e^{0.7}$
$O^+ + e \rightarrow O$	$4.43 \times 10^{-12}/T_e^{0.7}$
$N_2{}^+ + e \rightarrow N_2$	$1.80 \times 10^{-7}/T_e^{0.39}$
$NO^+ + e \rightarrow NO$	$4.20 \times 10^{-7}/T_e^{0.85}$
$O_2{}^+ + e \rightarrow O_2$	$1.60 \times 10^{-7}/T_e^{0.55}$

$$k_1 = 1.53 \times 10^{-12} - 5.92 \times 10^{-13} T_{300}(O^+) + 8.60 \times 10^{-14} T_{300}^2(O^+) \text{ for } T(O^+) < 1700K$$

$$k_1 = 1.73 \times 10^{-12} - 1.16 \times 10^{-12} T_{300}(O^+) + 1.48 \times 10^{-13} T_{300}^2(O^+) \text{ for } T(O^+) > 1700K$$

$$k_2 = 2.82 \times 10^{-11} - 7.74 \times 10^{-12} T_{300}(O^+) + 1.07 \times 10^{-12} T_{300}^2(O^+) - 5.17 \times 10^{-14} T_{300}^3(O^+) + 9.65 \times 10^{-16} T_{300}^4(O^+)$$

$$T_{300} = T/300$$

MAGNETIC FIELD

- appropriate field: IGRF
- modeled as a tilted (offset) dipole field, or IGRF-like
- low- to mid-latitude:
  closed field lines
- high latitude:
  open field lines
- important assumption:
  field lines are equipotentials

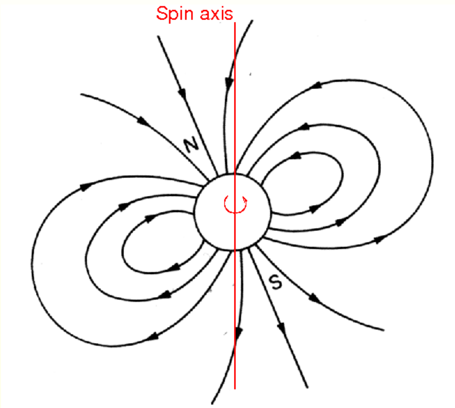

ELECTRIC FIELD

- Low latiutde: driven by neutral wind
    - empirical models (e.g., Fejer-Scherliess)
    - self-consistently determined (e.g., Eccles, Richmond)
- high latitude: driven by solar wind/magnetosphere currents
    - empirical models (e.g., Heppner-Maynard)
    - self-consistently determined from global magnetospheric models (e.g., LFM, RCM)

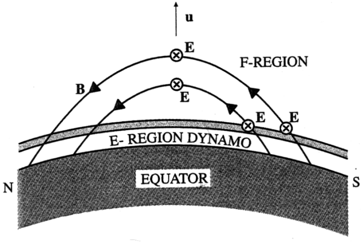

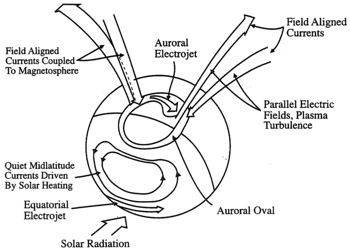

ELECTRODYNAMIC COUPLING

based on current conservation

$$\nabla \cdot \mathbf{J} = 0 \quad \mathbf{J} = \sigma \mathbf{E} \quad \rightarrow \quad \nabla \cdot \sigma \mathbf{E} = 0$$

Field-line integration: $\int \nabla \cdot \sigma \mathbf{E} \, ds = 0$

$$\nabla \cdot \mathbf{\Sigma} \nabla \Phi = S(J_{\|}, V_n, ...)$$

$$\mathbf{E} = -\nabla \Phi$$

- Σ: field-line integrated Hall and Pedersen conductivities
- $J_{\|}$: magnetosphere driven
- V_n: solar and magnetosphere driven

HOW IS THE MODEL BUILT?

- transport
  - parallel
  - perpendicular
- grid
  - lagrangian
  - eulerian

- continuity equation

$$\frac{\partial n_i}{\partial t} + \nabla \cdot (n_i \mathbf{V}_i) = P_i - L_i n_i$$

$$\frac{\partial n_i}{\partial t} + \nabla_\parallel \cdot \left(n_i \mathbf{V}_{i\parallel}\right) + \nabla \cdot (n_i \mathbf{V}_{i\perp}) = P_i - L_i n_i$$

  - parallel motion (diffusion/advection)

$$\frac{\partial n_i}{\partial t} + \nabla_\parallel \cdot \left(n_i \mathbf{V}_{\parallel i}\right) = P_i - L_i n_i \quad \text{for} \quad t \stackrel{\Delta t}{\rightarrow} t*$$

  - perpendicular motion (advection)

$$\frac{\partial n_i}{\partial t} + \nabla \cdot (n_i \mathbf{V}_{\perp i}) = 0 \quad \text{for} \quad t* \stackrel{\Delta t}{\rightarrow} t + \Delta t$$

PARALLEL TRANSPORT

conventional method: ignore ion inertia

$$\frac{\partial n_i}{\partial t} + b_s^2 \frac{\partial}{\partial s} \frac{n_i V_{is}}{b_s} = P_i - L_i n_i$$

$$0 = -\frac{1}{n_i m_i} b_s \frac{\partial (P_i + P_e)}{\partial s} + g_s - \nu_{in}(V_{is} - V_{ns}) - \sum_j \nu_{ij}(V_{is} - V_{js})$$

- procedure:
  $\longrightarrow$ solve for ion velocity V_{is}
  $\longrightarrow$ substitute into continuity
  $\longrightarrow$ expand density $n_i \simeq n_{i0} + n_{i1}$
  $\longrightarrow$ obtain fully implicit differencing scheme
  $\longrightarrow$ iterate equations to obtain a solution
- advantage: large time steps ($\sim$ 5 – 15 min)
- disadvantage: complexity, stability, limited species (e.g., no molecular transport)

PARALLEL TRANSPORT

SAMI2/3 method: include ion inertia

$$\frac{\partial n_i}{\partial t} + b_s^2 \frac{\partial}{\partial s} \frac{n_i V_{is}}{b_s} = P_i - L_i n_i$$

$$\frac{\partial V_{is}}{\partial t} + (\mathbf{V}_i \cdot \nabla) V_{is} = -\frac{1}{n_i m_i} b_s \frac{\partial (P_i + P_e)}{\partial s} + g_s - \nu_{in}(V_{is} - V_{ns}) - \sum_j \nu_{ij}(V_{is} - V_{js})$$

- procedure:
  $\rightarrow$ diffusion terms backward biased (implicit)
  $\rightarrow$ advection terms use donor cell method
  $\rightarrow$ obtain semi-implicit differencing scheme
- disadvantage: small time steps ($\sim$ 1 – 15 sec)
- advantage: simplicity, stability, flexibility, better description at high altitudes

PERPENDICULAR TRANSPORT

- perpendicular dynamics ($E \times B$ transport)
  - lagrangian grid: follow flux tube motion
  - eulerian grid: fixed mesh

LAGRANGIAN GRID

Follow $E \times B$ drift of a flux tube

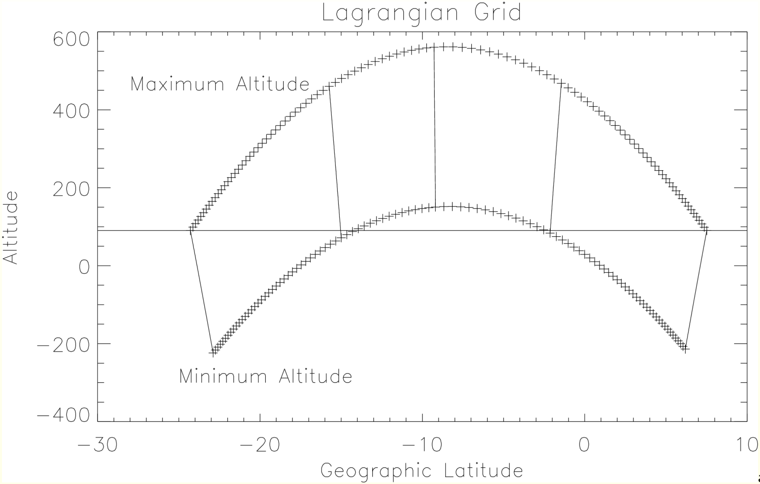

animate

EULERIAN GRID

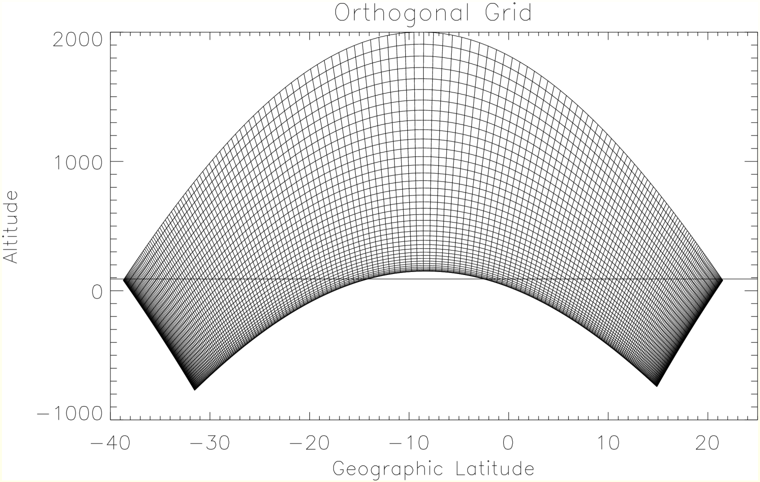

EULERIAN GRID

nonorthogonal: finite volume, donor cell method

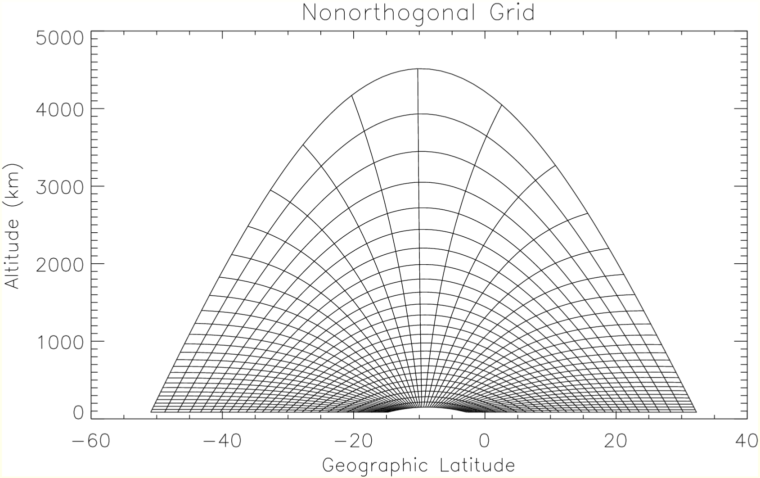

GRID COMPARISON

lagrangian, orthogonal eulerian, nonorthogonal eulerian

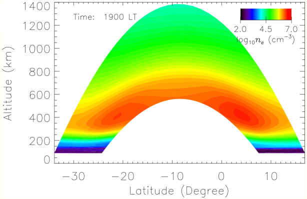

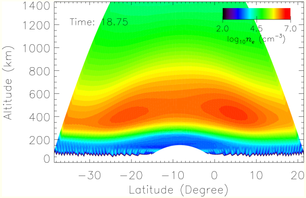

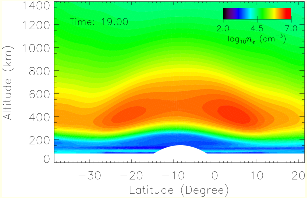

OVERVIEW OF SAMI2

- magnetic field: Offset, tilted dipole model / IGRF-like
- interhemispheric / global $\pm 60^\circ$
- nonorthogonal, nonuniform fixed grid
- seven (7) ion species (all ions are equal):
  H^+, He^+, N^+, O^+, N_2^+, NO^+, and O_2^+
  - solve continuity and momentum for all 7 species
  - solve temperature for H^+, He^+, O^+, and e^-
- plasma motion
  - $\mathbf{E} \times \mathbf{B}$ drift perpendicular to **B**
    (both vertical and longitudinal in SAMI3)
  - ion inertia included parallel to **B**
- neutral species: NRLMSISE00/HWM93/HWM07 and TIMEGCM
- chemistry: 21 reactions + recombination
- photoionization: daytime and nighttime

ELECTRON HEATING EQUATION

- electron temperature

$$\frac{\partial T_e}{\partial t} - \frac{2}{3}\frac{1}{n_e k} b_s^2 \frac{\partial}{\partial s} \kappa_e \frac{\partial T_e}{\partial s} = Q_{en} + Q_{ei} + Q_{phe} + Q_{RF}$$

- source term

$$Q_{source} = \left(\frac{dT_e}{dt}\right)_0 \exp[-(z - z_0)^2/\Delta z^2] \exp[-(\theta - \theta_0)^2/\Delta\theta^2]$$

- parameters
  - $(dT_e/dt)_0 = 1000$ K/s
  - $z_0 = 290$ km; $\Delta z = 40$ km (F10.7 = 100)
  - $z_0 = 275$ km; $\Delta z = 40$ km (F10.7 = 120)
  - $\theta_0 = 18.3°$; $\Delta\theta = 0.25°$

SAMI2 MODIFICATION

subroutine etemp(tte,te_old,phprodr,nfl,hrut)

```
nzh = ( nz - 1 ) / 2

do i = nzh,nz
  s6e(i) = 0.
  hrl = mod(hrut + glons(nz,nfl) / 15.,24.)
  if ( hrl .gt. theat_on .and. hrl .lt. theat_off ) then
    argt0  =(alts(i,nfl)  - alt0) / delalt
    argt1  =(glats(i,nfl) - lat0) / dellat
    s6e(i) =terate*exp(-argt0 * argt0)*exp(-argt1*argt1)
  endif
enddo

call tesolv(tte,te_old,kape,s1e,s2e,s3e,s4e,s5e,s6e,nfl)
```

PREVIOUS WORK

emphasis: local effects not conjugate

- Perrine, R.P., G. Milikh, K. Papadopoulos, J.D. Huba, G. Joyce, M. Swisdak, and Y. Dimant, An interhemispheric model of artificial ionospheric ducts, *Radio Sci. 41*, RS4002, doi:10.1029/2005RS003371, 2006.
- Milikh, G.M., A.G. Demekhov, K. Papadopoulos, A. Vartanyan, J.D. Huba, and G. Joyce, Model of artificial ionospheric ducts due to HF-heating, to be published in *Geophys. Res. Lett.*, 2010.

SURA

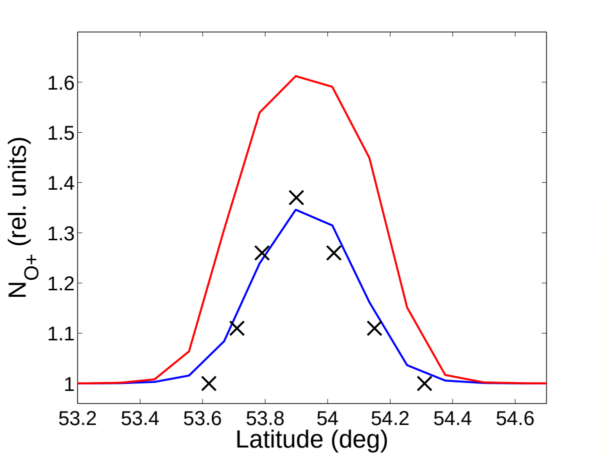
1.6
1.5
1.4
1.3
1.2
1.1
1
53.2
53.4
53.6
53.8
54
54.2
54.4
54.6
Latitude (deg)
N_{O+} (rel. units)

ELECTRON TEMPERATURE

F10.7 = 100

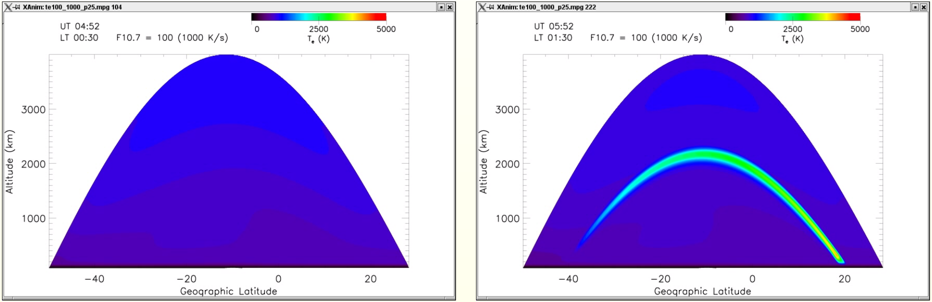

ELECTRON TEMPERATURE

F10.7 = 100

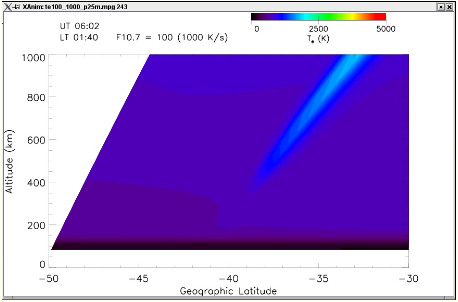

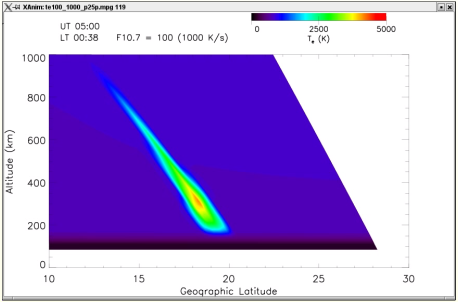

ELECTRON DENSITY

F10.7 = 100

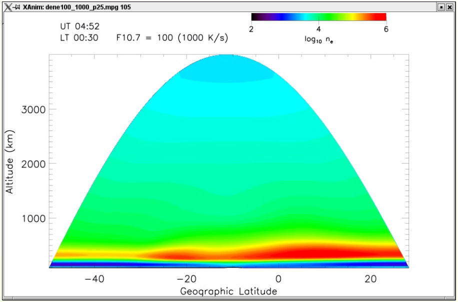

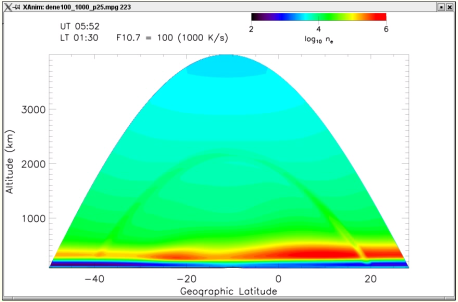

ELECTRON DENSITY

F10.7 = 100

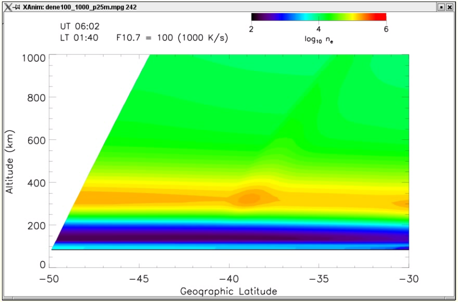

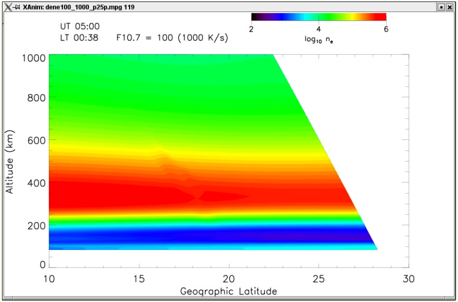

ELECTRON TEMPERATURE

F10.7 = 100

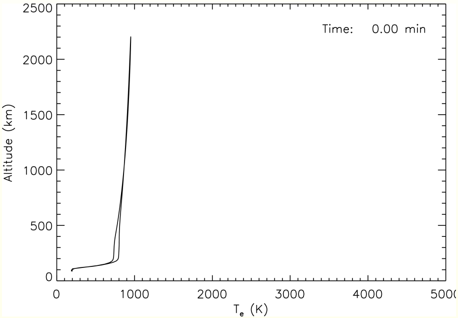

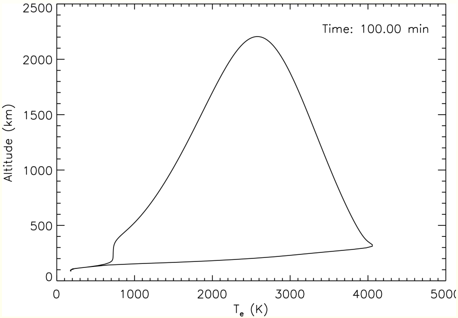

ELECTRON DENSITY

F10.7 = 100

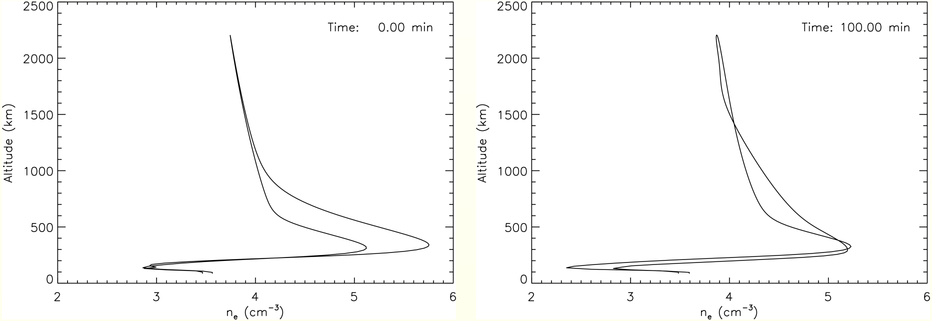

ELECTRON TEMPERATURE AND DENSITY

F10.7 = 120

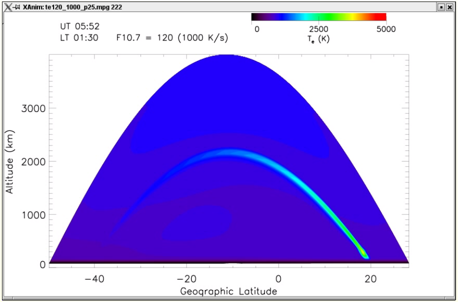

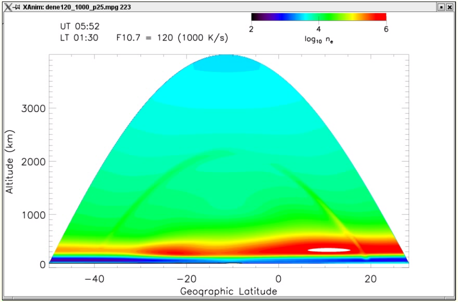

ELECTRON TEMPERATURE AND DENSITY

versus time (F10.7 = 100)

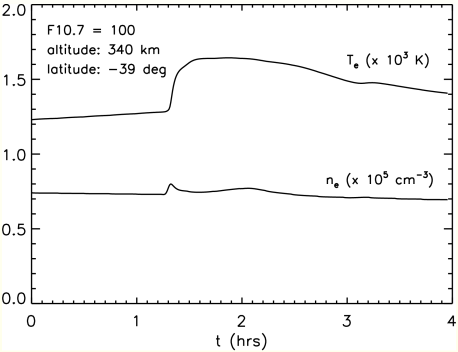

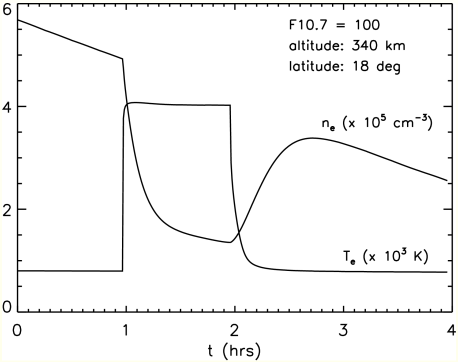

ELECTRON TEMPERATURE AND DENSITY

versus time (F10.7 = 120)

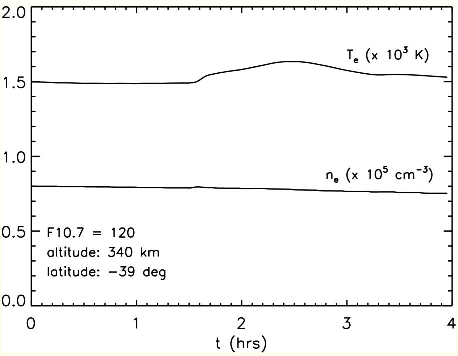

PRELIMINARY CONCLUSIONS

- electron density and temperature enhancements should be observable in the conjugate ionosphere during arecibo heating experiments (satellite and ground based measurements)
- we find the topside electron temperature can increase by $\sim 33\%$ and the electron density by $\sim 10\%$
- conjugate effects largest for relatively thin F layers, i.e., post-midnight
- further, more detailed simulations warranted
  - 3D SAMI3 simulations with zonal winds
  - more accurate heating algorithm